Plio-Pleistocene stratigraphic sequences and depositional model using 3D seismic interpretation constrained by well logs in Central Graben, North Sea

Haris Ahmed Khan[1], Taher Zouaghi[2,3,*], Shaista Iftekhar[1], Muhammad Jahangir Khan[1] and Muhammad Irfan[1]

[1] *Department of Earth and Environmental Sciences, Bahria University, Karachi Campus, 13 National Stadium Road, Karachi 75260, Pakistan.*
[2] *Department of Geoexploration, Faculty of Earth Sciences, King Abdulaziz University, Jeddah 21589, Saudi Arabia.*
[3] *Laboratoire de Géoressources, CERTE, Pôle Technologique de BorjCédria, 8020 Soliman, Tunisia.*
Corresponding author. e-mail: taher.zouaghi@kau.edu.sa; taher.zouaghi2018@gmail.com

This work presents depositional and structural model of Plio-Pleistocene delta of southern Central Graben offshore basin of Netherlands, based on seismic reflections and well logs tools. The studied interval of the Plio-Pleistocene delta is divided into 5 seismic super units, 11 seismic units, and 24 seismic subunits. Seismic reflections were correlated with the wire line records that lead to identification of depositional sequences and parasequences. The seismic units contain 27 well log units interpreted as depositional sequences. Each depositional sequence in term is composed of component parasequences corresponding to progradational and aggradational/retrogradational systems tracts. The main regional interpreted units can be correlated with the regional seismo-stratigraphy, chrono-eustatic and chronostratigraphy. Other previous works show that the Mid-Miocene to top Pleistocene interval is divided regionally into 13 seismic units and 18 log units. Coastline shifting and the sediment supply direction through Plio-Pleistocene time have been detected by lateral changes in clinoform geometry captured via construction of seismic unit's time structure maps. Seismic super unit and seismic unit boundaries have been delineated by onlaps, downlaps, toplaps, truncations of seismic reflectors, which show the significant landward and basinward shifting of coastline. Boundaries of seismic subunits are marked on the basis of depositional cycles. Depositional cycles are characterized on the basis of gamma ray log trends (funnel shape, bell shape, and cylindrical shape) and their associated geometry of parasequences (lowstand, transgressive, and highstand, systems tracts). This work results in a sequential and geometric characterization of the defined deep-seated sedimentary units. It provides a better comprehension of the sedimentary, eustatic, and geodynamic evolution of the North Sea domains, and consequently a better evaluation of its economic interests.

Keywords. Plio-Pleistocene; North Sea; seismic stratigraphy; wire-line; depositional sequence; delta geometry.

1. Introduction

The North Sea basin located at North Atlantic inland margin (Anell *et al.* 2010; Stuart and Huuse 2012), covers about 625,000 km^2 area. The North Sea is bounded from the east, south and west by Norway, Denmark, Germany, Netherland, Belgium, and United Kingdom, respectively (figure 1) and from the north it is bounded by Shetland Islands and Norwegian Sea (Ritsema and Gurpinar 2012). Due to the periodic phases of Variscan orogeny and Mesozoic failed rift system, North Sea subsurface is dominated by grabens/sub-basins (Van Wijhe 1987; Leeder 2009). Grabens/sub-basins perceived inversion during Late Cretaceous and Eocene (Glennie 2009) and tensional phases from Oligocene and afterward are caused by the Alpine orogeny throughout the North Sea and Danish area, this rejuvenation is also responsible for the reactivation of some grabens (Ziegler 1990).

The Lower Rhine Graben oriented in southeast northwest direction towards the southern North Sea and Netherlands (Ritsema and Gurpinar 2012). North Sea Central Graben oriented in north-south direction (figure 1), ranging from the north of Netherlands offshore to the north of Norway offshore (Abbink *et al.* 2006). The Viking Graben oriented in southeast direction, along the Norwegian coast (Ziegler 1990). Comparatively two smaller grabens Horn Graben and Terschelling Graben are present in the east and south of Central Graben, respectively. The Horn Graben and the Terschelling Graben are both found north of the Netherlands' coast.

This study deals with the implication of sequence stratigraphic concept on F3-block wave-dominated delta of Plio-Pleistocene age. Application of sequence stratigraphy helps to understand the depositional geometry and process (basin filling, erosion, truncation, traps, seal, source and reservoir spatial distribution), environmental settings (systems tracts) and lithology prediction (Vail 1987). Sequences and systems tracts are delineated based on seismic discontinuities and reflection terminations (toplap, downlap, onlap and truncation) to understand the sea-level changes, rate of sedimentation with respect to accommodation and environment of deposition. It will add to seismic and sequence stratigraphic interpretations that have been done in the past (Lacaze *et al.* 2011).

Aim of this research was to delineate the seismic subunits to understand the evolution of Plio-Pleistocene delta. Nevertheless, in future the extension of this research shall be the accurate estimation and target the shallow potential stratigraphic gas traps.

2. Geological setting

The Central European Basins system has undergone Variscan orogeny of Paleozoic, Jurassic failed rift and Alpine orogeny pulses from Oligocene to onwards. The Variscan orogeny related deformations of North Atlantic domain, including North Sea, commenced during Late Carboniferous and continued until Early Triassic (Haszeldine and Russell 1987; Lyngsie and Thybo 2007; Anell *et al.* 2010). This basin further developed under the load of deformational front advancement into the foreland basin (Ziegler and Cloetingh 2004). The Ringkobing-Fyn high appears during the Asturian pulse of Variscan orogeny and separates the basin into two parts southern North Sea and northern North Sea basins. During Late Triassic, several sub-basins were formed within the southern Permian Basin by the extensional tectonism related to differential vertical motions. The substantial rifting began in Late Jurassic and ended in the Early Cretaceous (Ziegler 1990; Anell *et al.* 2010) and during this period formation of Grabens happened within the North Sea region (Van Wijhe 1987).

The counter-clockwise movement of African plate throughout Cenozoic era and the phases of Alpine orogeny deliver transpressional stress on North Sea Basins (Rasser *et al.* 2008) that resulted into periodic inversion (reversed the basins bounding faults) of the basins (Van Wijhe 1987; Ziegler 1987, 1988, 1990; Dronkers and Mrozek 1991; Ziegler *et al.* 1995; Marotta *et al.* 2002; Knox *et al.* 2010). The inversion of the Dutch basins is dominated by the two additional pulses of Alpine orogeny, one ends at Eocene–Oligocene border and the other ends at Oligocene–Miocene border (De Jager 2003).

The Cenozoic sediments mainly consist of marine clay and sands (figure 2). The North Sea Groups of Cenozoic era, approximately 1460 m in total thickness unconformably overlying the Chalk Group of Late Cretaceous. In North Sea region thermally subsiding basin (epicontinental basin received sediments from neighboring landmasses), were formed during Cenozoic era (Sclater and Christie 1980; Ziegler 1988; Jordt *et al.* 1995; Sørensen *et al.* 1997; Faleide *et al.* 2002; Tetyukhina *et al.* 2010; Benvenuti *et al.* 2012; Mojeddifar *et al.* 2015;
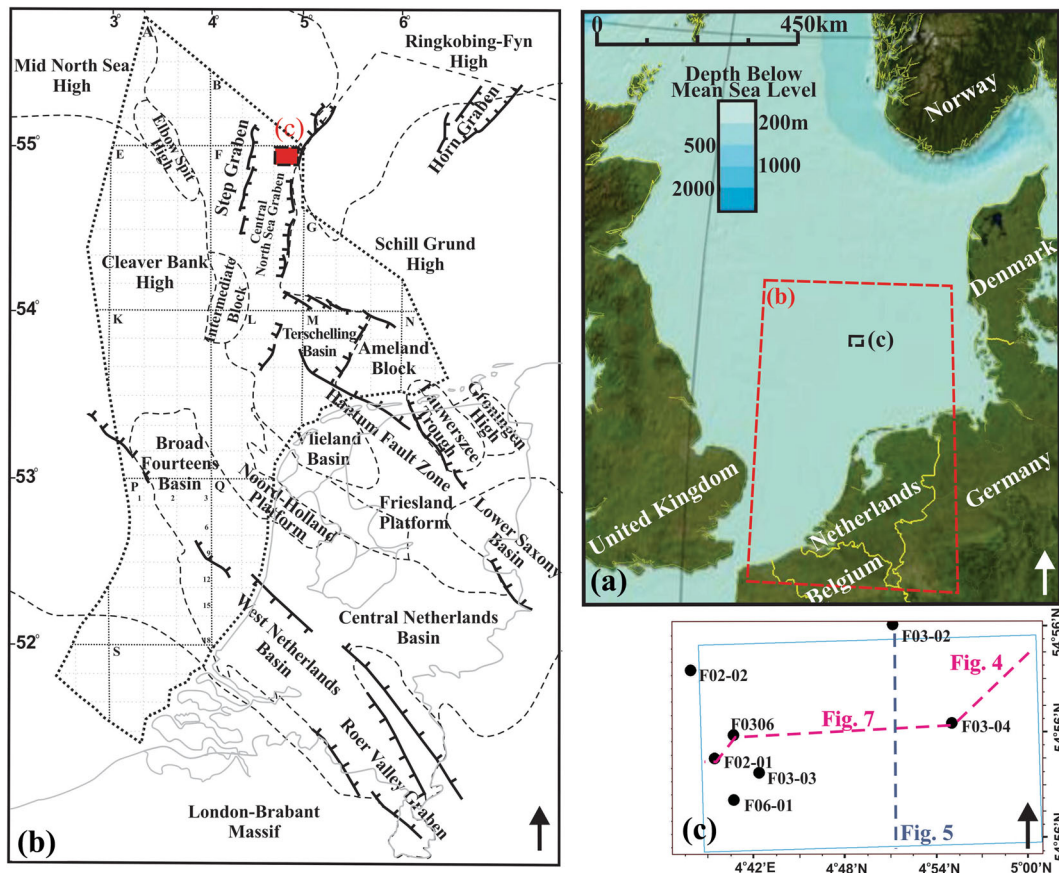
Figure 1. Location map of F3-block: **(a)** subset of coordinate reference system ED50-UTM31, **(b)** Netherlands onshore and offshore boundaries and structural elements of the Late Jurassic–Early Cretaceous, modified after (Schroot and Schüttenhelm 2003; Kombrink *et al.* 2012; Nelskamp *et al.* 2012), **(c)** the seismic survey boundary of F3-block in blue, the location of the wells by black dots and the north-south and east-west cross sections by dashed lines.

Figure 2. Stratigraphic column of Netherlands offshore Central Grabben Basin (CGB), modified after (Duin *et al.* 2006; Van Dalfsen *et al.* 2006).

Thöle *et al.* 2016). During Oligocene uplifting of Scandinavian shield fluvio-deltaic system started draining, which is responsible for the development of sequences in northwestern Europe region and offshore region of Dutch Sector (southern embayment) (Bijlsma 1981; Rohrman *et al.* 1995, 1996). The southern North Sea basin received

Neogene to Pleistocene sediments through north German rivers that drained westward (Zagwijn 1974). During Late Miocene and Early Pliocene rate of uplifting of Fennoscandia hinterland increased (Ghazi 1992; Sales 1992; Jordt *et al.* 1995) and the drainage system shifted from Danish (northeast and east) to southern embayment

(Spjeldnaes 1975) throughout this time the rate of sedimentation exceeded the rate of subsidence and the basin shallowing occurred.

Uplifting rate of Fennoscandian shield supposedly increased during Miocene (Jordt *et al.* 1995; Rundberg and Eidvin 2005; Rasmussen *et al.* 2013). The differential load has been spread over the region due to the increasing load of sediments from Fennoscandian shield to North Sea Basin (Clausen *et al.* 2012, 2013; Harding and Huuse 2015). This caused rapid subsidence in basin center and minor subsidence or even uplifting at basin margin (Kooi *et al.* 1991; Cloetingh *et al.* 1992) because of this Zechstein salt of Permian age began to move and formed numerous unconformities within Pliocene interval (Qayyum *et al.* 2013).

Ringkobing-Fyn high of Permian age reactivates during Middle Miocene to Pliocene times and partly detached the North Sea Basin into northern embayment and southern embayment (Sørensen and Michelsen 1995). Inwards the west of deep seaway of Central Graben Basin these embayments were linked and depocentres were found within them (Sørensen *et al.* 1997). Northern embayment covers northern part of Central Graben Basin and Norwegian-Danish Basin, whereas southern embayment covers southern part of Central Graben Basin and North German Basin.

The rate of sedimentation drastically increased during Quaternary time; during 2% of Cenozoic deposition time interval, half of the total thickness was deposited (Van Wees and Cloetingh 1996). During glacial time subsidence accelerated and sediments deposited in fluvial and shallow marine conditions (De Gans 2007).

The Lower North Sea Group (LNSG) about 410 m thick consist of mainly marine shale and little portion of marl 40 m thick at the top (Winthaegen and Verweij 2003). The Middle North Sea Group (MNSG) about 350 m thick and the lithology of this group is mainly shale. The succession of Cenozoic era can also be separated into two packages by regionally marked Mid-Miocene unconformity (Deagan and Scull 1977; Kristoffersen and Bang 1982; Sørensen *et al.* 1997; Overeem *et al.* 2001; Winthaegen and Verweij 2003; Anell *et al.* 2010; Tetyukhina *et al.* 2010; Mojeddifar *et al.* 2015). The lower package primarily contains Paleogene sediments (Lower and Middle North Sea Groups), which are comparatively fine grained (Steeghs *et al.* 2000) than the upper package of Neogene sediments (Upper North Sea Group) about 700 m thick. Lithologically, Upper North Sea Group (UNSG) consists of coarser in grain size deltaic sandy-clay stone and sand, which exhibit complex geometries (Mojeddifar *et al.* 2015). The Pliocene uplift of Scandinavia triggered the regression that caused the large influx of coarse sediments into the North Sea (Gregersen *et al.* 1997; Eidvin and Rundberg 2001; Rasmussen and Dybkjaer 2005). The main direction of progradational deltaic sequence (clinoforms) of upper package is towards west-southwest (Tigrek 1998), which corresponds to the different phases of delta evolution.

3. Data set and methodology

3D post-stack time-migrated seismic grid data within the F3-block that covers about 380 km^2 area. Seismic grid consists of 947 X lines and 646 In lines with 25 m sampling interval in both directions and 4 m sampling rate. The base map (figure 1) shows the location of 7 available wells and the availability of well logs presented in table 1. Four wells F02-01, F03-02, F03-04 and F03-06 are selected (based on suitable location) to appraise the interpretation of this research.

Structural time map of interpreted seismic unit tops are also generated to recognize the delta front progress. Seismic and well log data has been integrated to understand the stacking patterns and depositional trends of the study area. Prior the data integration, both the data sets (seismic data in time and well log data in depth) interpreted individually and then calibrated to complement each other (Datta Gupta *et al.* 2012). Multiple techniques exist that allow to develop time–depth relation (Walden and White 1984; White 1997; White and Simm 2003; Duchesne and Gaillot 2011; Edgar and Van Der Baan 2011). Wavelet has been extracted to generate synthetic seismograms, at location of each well. The main purpose of this exercise is to identify the exact seismic horizons against the corresponding well tops (figure 3), and for this purpose Petrel software has been utilized to generate synthetic seismogram. Their interfaces allow us to starch and squeeze generated synthetic seismogram for the best match with seismic traces (Munoz and Hale 2012). All types of data sets provide different insights (Catuneanu *et al.* 2009), and precise calibration broaden the understanding about the given data. Keeping this in view synthetic seismogram is generated on zero-phase Ricker wavelet of 40 Hz, 2 m sampling rate and normal polarity to achieve best seismic to well tie.

Table 1. *Tabulated presentation of available well and well logs.*

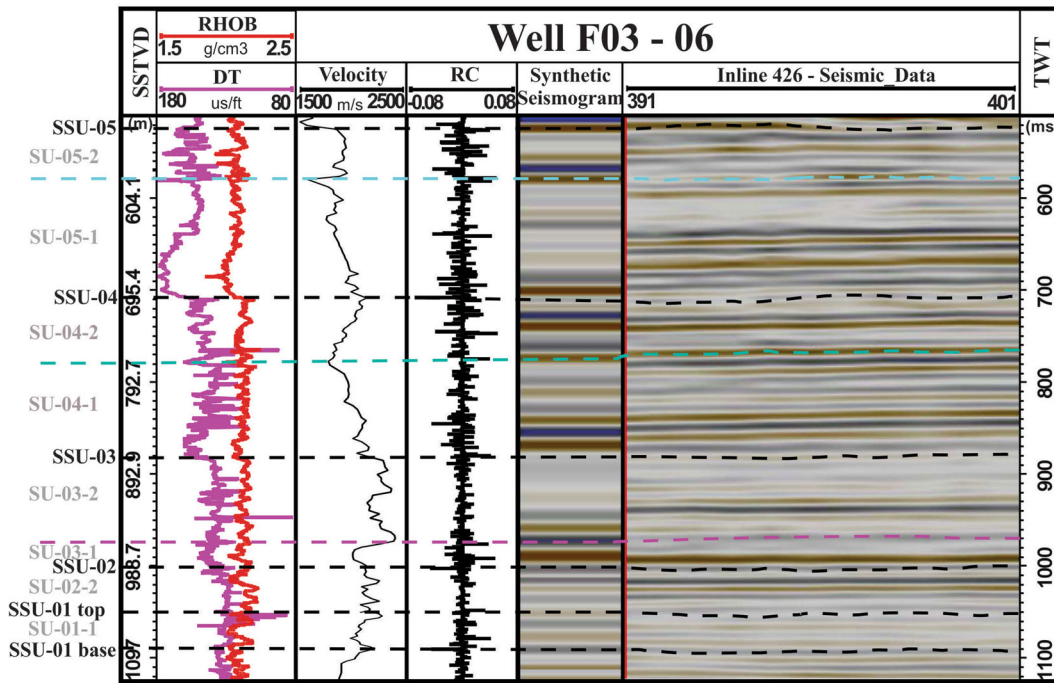| Wells	GR	SP	DT	RHOB	NPHI	PHIE	LLD	LLS	MSFL	SN	AI	AI_rel	Cali
F06-01	√	X	√	√	X	√	X	X	X	X	√	√	X
F02-01	√	√	√	√	√	√	√	√	√	√	√	√	X
F03-02	√	X	√	√	X	√	X	X	X	X	√	√	X
F03-04	√	√	√	√	X	√	X	X	X	X	√	√	X
F03-06	√	√	√	√	√	X	√	√	√	X	X	X	√
F03-03	√	√	√	√	√	X	√	√	√	√	X	X	√
F02-02	√	X	√	√	X	X	X	X	X	X	X	X	X

Figure 3. Synthetic seismogram of well F03-06 was generated to choose the best fit wavelet for perfect correlation with seismic data. From left to right, depth (TVD) displayed within first track, sonic (DT) and density (RHOB) displayed within the second track by pink and red color respectively, Derived velocity (Vp) displayed with in the third track by thin black solid line. Reflection coefficient (Kooi *et al.* 1991) displayed within the fourth track. Synthetic tied with Inline 426 displayed within the fifth and sixth track respectively, and two-way travel time (TWT) within the seventh track.

The gamma ray is the only log available in all wells that correlates laterally and differentiate vertically between shale and sand layers within the study area. Luthi (2001) suggested to acquire the basic gamma ray log interpretation rule, that is the gamma ray lower values correspond to the sandy layers and inversely higher values to the shale/clay layers. Mojeddifar *et al.* (2015) interpret two types of lithology (sand and shale) and within three seismic units above the Mid-Miocene unconformity. The gamma ray log value above 70 API correspond to the shale rich sediments mainly belonging to the seismic unit 1 and 3. However, the gamma ray log value lower than 70 API correspond to the sand

rich sediments normally belongs to the seismic unit 2.

In this study, we further subdivided (Mojeddifar *et al.* 2015) seismic unit 2 into further 5 seismic super units, 11 seismic units and 24 seismic subunits, which represent the phases of deltaic evolution (figures 4–7). Four types of lithologies were interpreted based on the range of gamma ray log (figure 7). The gamma ray log value below 20 API is interpreted as coarse sand, between 20 and 45 API is sand, between 45 and 70 API is fine sand and above 70 API is shale.

Sequence stratigraphy is very strong tool (for correlating regional and local scales) to understand the stratigraphic evolution by integrating multiple
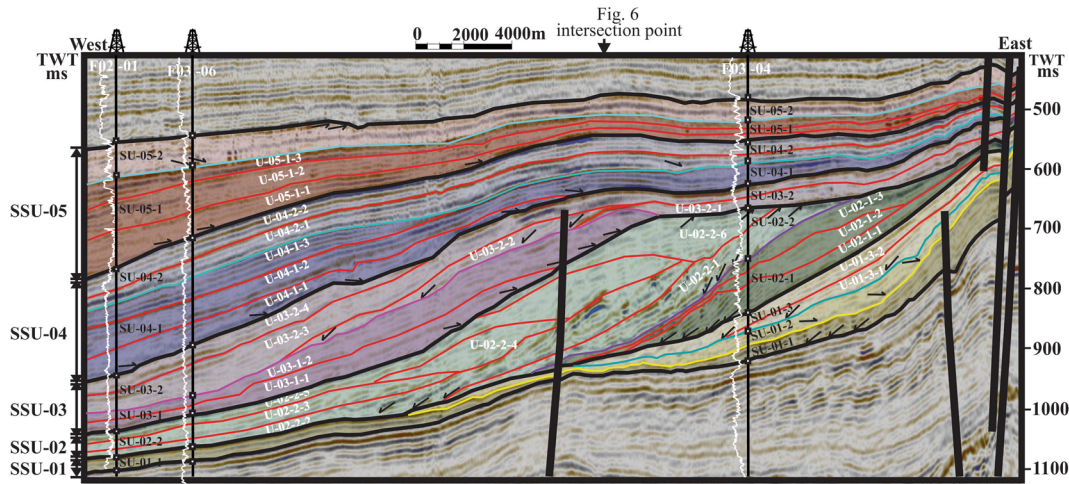
Figure 4. Interpreted arbitrary composite seismic section through wells from east-west direction, showing older to younger sequences (SSU-01- to SSU-05) depositional pattern, identify on the basis of onlapping, offlapping, toplapping and downlapping patterns of parasequences. Boundaries of seismic super units are marked by thick black color, seismic units are represented by specific color to differentiate, however seismic subunits are represented by red colour.
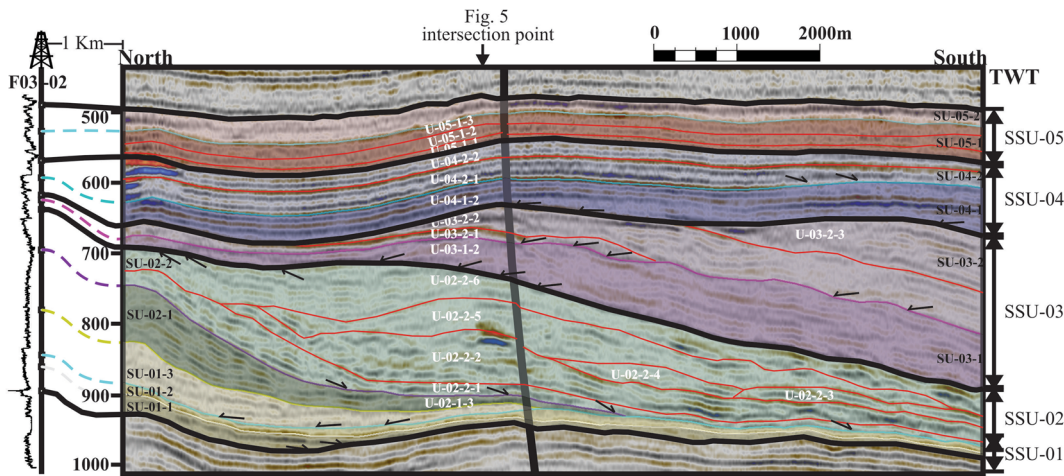

Figure 5. Interpreted Inline-847 seismic section from north-south direction, showing older to younger seismic super units (SSU-01- to SSU-05) depositional pattern, identify on the basis of onlapping, offlapping, toplapping and downlapping patterns of parasequences. Inline-847 selected to correlate it with the well F03-02, which exists at the distance ∼1 km from the section. Boundaries of seismic super units are marked by thick black color, seismic units are represented by specific color to differentiate, however seismic subunits are represented by red color.

sets of data (Catuneanu *et al.* 2009) for developing chronostratigraphic framework (Lacaze *et al.* 2011). Seismic sequence stratigraphy deals with the interpretation of the main reflection packages and further subdivision of these reflection packages into seismic sequences and systems tracts. The prograding delta succession (delta top and clinoform break) is illustrated in schematic diagram (figure 6a). The maximum isopach thickness of each SSU and SU is considered as the clinoform-containing delta front, which help to mark the approximate paleo-shoreline on maps (figure 6b) to understand the sediment supply direction.

Funnel shaped geometry of GR log indicates the shallowing upward (Das *et al.* 2017; Das and Chatterjee 2018) and forestepped accumulation pattern of parasequences during lowstand systems tract (LST). Deepening upward and fining upward strata interpreted by bell shape geometry of GR log during transgressive systems tract (TST) due to rise of relative sea level (figure 7). Funnel and/or cylindrical shape geometry of GR log indicates the thickening upward and coarsening upward strata was formed due to the prograding and/or aggrading accumulation pattern of parasequences (Zouaghi *et al.* 2011) during
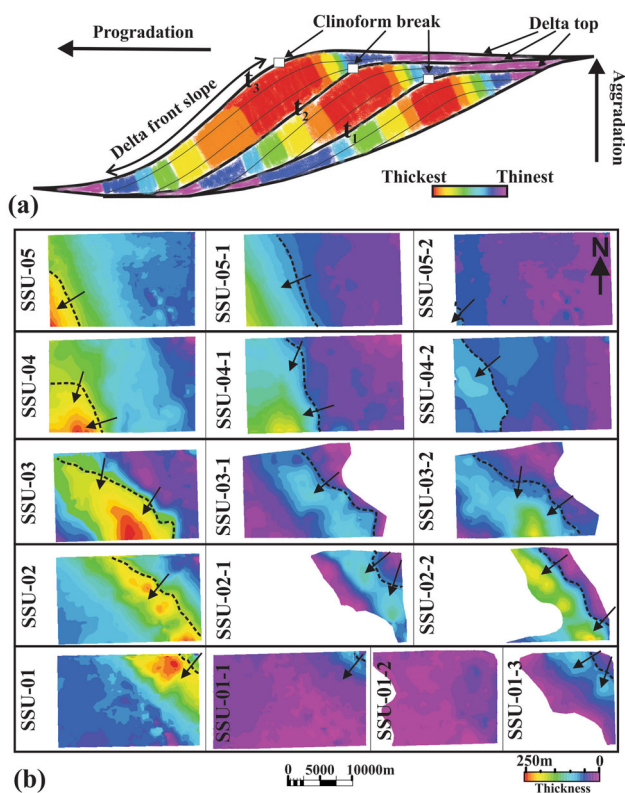
Figure 6. **(a)** Schematic diagram showing variation of thickness of prograding seismic units within the delta succession. Top of delta and clinoform break are represented by white squares, the thickest red sections correspond to the clinoform-containing delta fronts, **(b)** F3-block isopach maps of super seismic units and seismic units representing the sediments supply direction (delta progradation) specified by the black arrows from delta top to clinoform-break. Moreover, indicates the approximate delta front location marked dashed-black line.

highstand systems tract (HST) and is applied while interpreting the seismic units.

According to the sequence stratigraphy hierarchical order (Vail *et al.* 1977; Miall 2000), the studied package has been identified as deposits of fourth order cycle and further characterized into systems tracts. Zouaghi *et al.* (2011) show that thickening-upward, shallowing and coarsening-upward parasequences could characterize lowstand systems tracts or highstand systems tracts; however, thinning-upward, deepening-upward and fining upward parasequences are characterized as transgressive systems tracts.

4. Results

Five seismic super units (SSU-01 to SSU-05) of Plio-Pleistocene age were defined in the 3D seismic data. SSU limits correspond to major unconformities, which are calibrated by F02-011, F03-02,

F03-04 and F06-01 wells (figures 4, 5 and 7). The maximum GR log value, within the sequence boundaries, is interpreted as maximum flooding surfaces (mfs).

The analogy of F3-block is the nearby A-block southern North Sea, where Kuhlmann and Wong (2008) regionally interpreted 13 key horizons Plio-Pleistocene intervals as sequence boundaries (S1—S13).

In North Sea F3-block, the dipping trend of interpreted seismic units is from north-northeast, evident in the isopach map of SSU and SU (figure 6b). In each unit, delta front is identified as the thickest portion that shifts its direction from northeast to east-west with respect to the source of sediment supply.

Base of Pliocene seismic unit-01-1 (SU-01-1) of seismic super unit-01 (SSU-01) on seismic section is represented by high amplitude continuous reflectors, whereas the above reflections are comparatively diffused (figures 4 and 5). The top of Pleistocene seismic unit-05-2 (SU-05-2) of seismic super unit-05 (SSU-05) is characterized by the base of high amplitude sporadic package; contrary to this the reflections above the sporadic reflectors package are transparent.

4.1 *Seismic super unit-01 (SSU-01)*

Seismic super unit-01 encloses three seismic units and two seismic subunits. The lower and upper boundaries of SSU-01 are characterized by the downlapping parasequences (angular unconformities) of overlying seismic unit SU-01-1 and unit U-02-1-1 (figures 4 and 5).

4.1.1 *Seismic unit-01-1 (SU-01-1)*

The upper boundary of SU-01-1 marked on the basis of overlying onlapping parasequences of seismic unit-01-2. Seismic reflectors of SU-01-1 show high amplitude facies at the distal part and variable amplitude facies at the proximal and slope of the delta. Closer to the delta platform, the reflectors are nearly parallel to sub-parallel. The downlapping and offlapping of SU-01-1 parasequences indicates the prograding and forestepped accumulation pattern of parasequences due to fall of sea level. The isopach map of base and top of SU-01-1 indicates that sediment supply was from northeast (figure 6b).

Throughout the study area SU-01-1 (∼26 m thick) consists of single depositional sequence in all
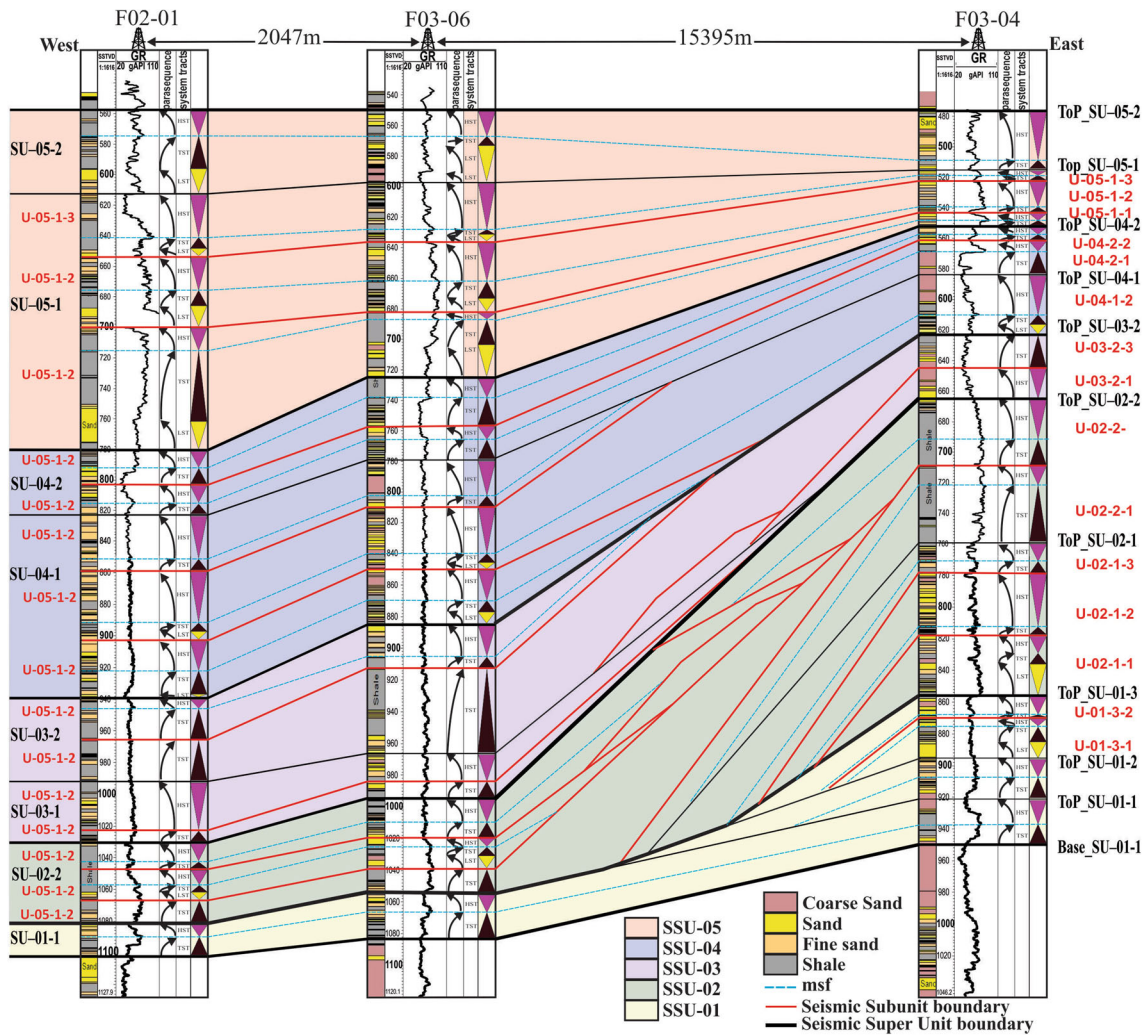
Figure 7. Wells section through east-west to correlate the seismic units and seismic subunits of Plio-Pleistocene delta. The recognized seismic super units are represented by different background colors and the boundaries are marked by heavy black lines, the seismic units are separated by thin black lines and the seismic subunits are represented by red color lines and maximum flooding surfaces by blue dashed lines. The geometry of U-02-2-4, U-02-2-5 and U-03-2-2 has been detected from the interpreted seismic sections of figures 4 and 5.

wells. The thickness of SU-01-1 slightly increases towards the northeastern uplifted region (figures 4 and 5). High and low, amplitude seismic reflections of this interval correspond to the low and high fluctuations of gamma ray (GR) response, respectively, of wells F02-01, F03-02, F03-06 and F03-04 (figure 7). Sand to shale (GR bell shape) shows retrograding of parasequences during TST and shale to coarse sand (GR funnel shape) was deposited afterward due to prograding parasequences during HST.

4.1.2 *Seismic unit-01-2 (SU-01-2)*

The upper boundary of SU-01-2 picked on the basis of overlying downlapping parasequences of

seismic unit-01-3 and unit U-02-2-2 (figure 4) westward (towards the slope) and the overlaying parasequences onlapping of SU-01-3 (figure 5) northeastward (towards the platform). Upper boundary of SU-01-2 shows moderate to low amplitude reflector. Towards the platform, reflectors are representing onlapping and in the westward direction, reflectors are pinching-out at the bottom of the slope. Figure 6(b) shows that SU-01-2 is restricted to the eastern portion of the study area. The onlapping of SU-01-2 parasequences towards the uplifted zone indicates the retrograding and back stepped accumulation pattern of parasequences due to the rise in sea level. The isopach map of SU-01-2 top indicates the no significant indication of sediment supply

direction due to spatial distribution of sediments restricted in the eastern portion of the study area (figure 6b).

Likewise, SU-01-1, seismic unit-01-2 (∼24 m thick) consists of single depositional sequence encounter in well F03-04 and F03-02, thickness of this seismic unit also slightly increases towards the northeastern uplifted region (figures 4 and 5). SU-01-2 shows coarse sand to fine sand (GR bell shape) indicates retrograding parasequences during TST (figure 7). In later stages of SU-01-2 aggrading parasequences during HST shows fine sand (GR cylindrical shape).

4.1.3 *Seismic unit-01-3 (SU-01-3)*

The upper boundary of SU-01-3 is the upper boundary of SSU-01 and the seismic reflectors of SU-01-3 show moderate reflection near the uplifted portion and low amplitude continuous reflector towards the slope. Reflectors are parallel to sub-parallel at the level of platform, however in western direction at the bottom of the slope reflectors are pinching-out. The onlapping and downlapping of SU-01-3 parasequences form near the platform and the slope, respectively, indicates the slope-fan accumulation pattern of parasequences due to fall of sea level (figures 4 and 5). SU-01-3 isopach map indicates two sediment supply directions from north-northeast and northeast (figure 6b).

The SU-01-3 sequence contains two seismic subunits (U-01-3-1 and U-01-3-2), which are restricted in northeastern region and encounters in well F03-04 and F03-02.

The thickness of U-01-3-1 gradually increases towards the northeastern uplifted region (figures 4 and 5). Seismic unit U-01-3-1 (∼23 m thick) has fine sand to thick sand deposits (GR funnel shape) due to prograding parasequences during LST. U-01-3-1 indicates sand to shale accumulation (GR bell shape) during TST (figure 7) and shale to sand accumulation (GR funnel shape) indicating prograding parasequences during HST.

However, the upper seismic subunit U-01-3-2 (∼14 m thick) indicates sand to fine sand (GR bell shape) due to retrograding parasequences during TST (figure 7). Sand to coarse sand (GR funnel shape) indicates prograding parasequences during HST.

4.2 *Seismic super unit-02 (SSU-02)*

Seismic super unit-02 comprises two seismic units and nine seismic subunits. The upper boundaries of SSU-02 are characterized by the toplapping of underlying seismic subunit U-02-2-6 and onlapping of overlying units of SU-03-1 (figures 4 and 5).

4.2.1 *Seismic unit-02-1 (SU-02-1)*

Seismic unit-02-1 bounded from top by overlying parasequences downlapping of U-02-2-1. Seismic reflectors of SU-02-1 shows low amplitude discontinuous reflection near the uplifted portion and high amplitude continuous reflector towards the slope and developing clinoform geometry (figure 8). The onlapping and downlapping of SU-02-1 parasequences form near the platform and the slope, respectively, due to the fall of sea level (figures 4 and 5). SU-02-1 top isopach map indicates the sediment supply diverged from northeast (figure 6b). The SU-02-1 sequence contains three seismic subunits (U-02-1-1, U-02-1-2 and U-02-1-3), which are restricted in northeast region and encounters only in wells F03-04 and F03-02.

The lower seismic subunit U-02-1-1 (∼38 m thick) overlaying the U-01-3-2, indicates shale to coarse sand (GR funnel shape) due to prograding parasequences during LST. Coarse sand to shale (GR bell shape) in this subunit shows retrograding parasequences during TST (figure 7). Shale to sand (GR funnel shape) within this subunit shows prograding parasequences during HST.

However, the middle seismic subunit U-02-1-2 (∼40 m thick) consists of sand to shale (GR bell shape) due to retrograding parasequences during TST (figure 7). It is followed by fine sand to coarse sand (GR cylindrical) due to aggrading pattern of parasequences during HST. The upper seismic subunit U-02-1-3 (∼18 m thick) is consists of fine sand to shale (GR bell shape) indicates retrograding parasequences during TST (figure 7). Afterward, sand and coarse sand is present (GR funnel shape) due to prograding parasequences during HST.

4.2.2 *Seismic unit-02-2 (SU-02-2)*

The upper boundary of SU-02-2 is the upper boundary of SSU-02 and the seismic reflectors of SU-02-2 shows moderate amplitude and prominent continuous reflection in overall studied area. The high angle downlapping pattern over the lower
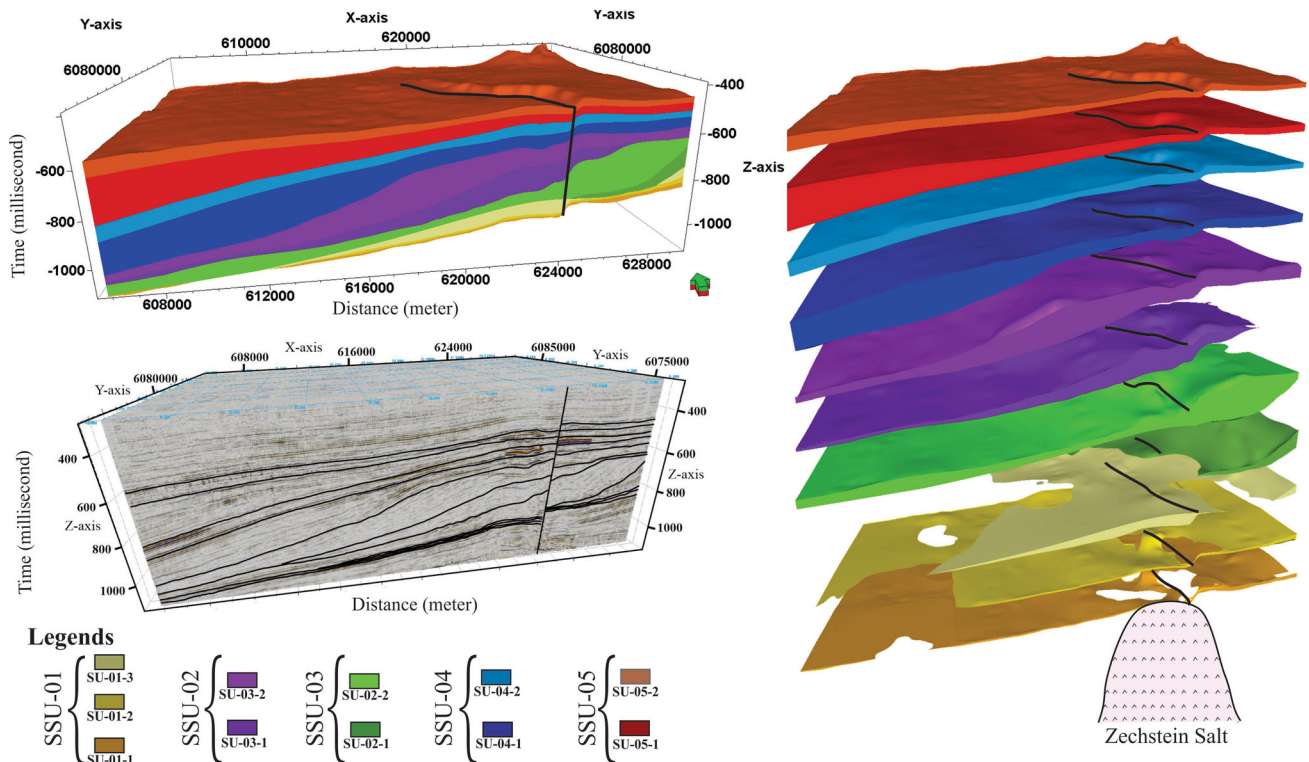
Figure 8. Structural geometry of NE to SW prograding Plio-Plistocene delta of North Sea F3-block.

boundary of SU-02-2 indicates the high sediment influx and low accommodation space deposition. The thickness of SU-02-2 increases towards the slope and gradually decreases towards the platform and basinward direction (figures 4 and 5). The sediment supply of SU-02-2 is northeast direction (figure 6).

The SU-02-2 sequence contains six seismic subunits (U-02-2-1 to SU-02-2-6), seismic subunits SU-U-02-2-2, U-02-2-3 and U-02-2-5, which encounters in western wells (F02-01 and F03-06). However, seismic subunits U-02-2-1 and U-02-2-6 encounter in eastern wells (F03-04 and F03-02) and are well developed over the slope. The seismic subunit U-02-2-4 is restricted in the middle portion of the studied area, also well developed over the slope, marked on the basis of onlapping and downlapping pattern of parasequences (figures 4 and 5).

The lower seismic subunit U-02-2-1 (∼52 m thick) overlaying the SU-02-1, consists of fine sand to shale (GR bell shape) due to retrograding pattern of parasequences during TST (figure 7). It is followed by shale to sand (GR funnel shape) deposited during prograding parasequences during HST.

The seismic subunit U-02-2-2 (∼14 m thick towards western direction in wells F02-01 and F03-06 and thickness increasing towards the

eastern part) consists of fine sand to shale (GR bell shape) due to prograding parasequences during TST.

Seismic subunit U-02-2-3 (∼20 m thick) consists of shale to sand (GR funnel shape) due to retrograding parasequences during LST. Sand to shale is present (abrupt change in GR) indicating retrograding parasequences during TST. Shale to sand (GR funnel shape) in this subunit indicates prograding parasequences during HST (figure 7).

The seismic subunit U-02-2-4 is limited in the middle part over the slope and pinching out prior to reach any of the studied well, due to this reason systems tracts of this seismic subunit are not picked.

Seismic subunit U-02-2-5 (∼15 m thick towards western direction in wells F02-01 and ∼24 m thick F03-06 and thickness increasing towards the eastern part) capping U-02-2-4 and pitched-out eastward over the seismic subunit U-02-2-2. This seismic subunit (U-02-2-5) consists of sand to shale (GR bell shape) due to retrograding of parasequences during TST. It is followed by shale to fine sand (GR cylindrical to funnel) due to aggrading parasequences during HST (figure 7).

Top most seismic subunit U-02-2-6 (∼44 m thick towards eastern direction in well F03-04 and thickness increasing towards the slope) limited in the

eastern part of the studied region and consists of shale (GR bell shape) due to retrograding parasequences during TST. Shale to sand (GR funnel shape) due to prograding parasequences during HST (figure 7).

4.3 *Seismic super unit-03 (SSU-03)*

Seismic super unit-03 comprises two seismic units and six seismic subunits. The upper boundaries of SSU-03 are characterized by onlapping of the overlying unit U-04-1-1 (figures 4 and 5).

4.3.1 *Seismic unit-03-1 (SU-03-1)*

The upper boundary of seismic unit SU-03-1is marked by the downlapping of overlying parasequences (angular unconformity) of U-03-2-2 (figures 4 and 5). Seismic reflectors of SU-03-1 show moderate to low reflections in overall region on east-west and north-south seismic line (figures 4 and 5). The thickness of SU-03-1 increases towards the slope and southward direction and gradually decreases towards the platform (northeast) and basinward in western direction (figures 4 and 5). SU-03-1 isopach map indicates the sediment supply from northeast (figure 6b). Offlapping arrangement of seismic units SU-02-1, SU-02-2 and SU-03-1 illustrate the fall of sea level, clearly visible in figures 4 and 5.

The SU-03-1 sequence contains two seismic subunits (U-03-1-1 and U-03-1-2), all the seismic subunit encounters only in western and northern wells (F02-01, F03-06, and F03-02) due to pinching out of SU-03-1 in eastern direction prior to reach at the level of platform (figures 4 and 7).

The lower seismic subunit U-03-1-1 ($\sim$8 m thick in well F02-01 and $\sim$11 m thick in F03-06) consists of fine sand to shale (GR bell shape) showing retrograding of parasequences during TST (figure 7).

The upper seismic subunit U-03-1-2 ($\sim$28 m thick in well F02-01 and this thickness decreasing toward eastern part, encounter $\sim$18 m thick in F03-06 well) consists of shale to sand (GR funnel shape) indicating prograding parasequences during HST.

4.3.2 *Seismic unit-03-2 (SU-03-2)*

The upper boundary of seismic unit-03-2 is the upper boundary of SSU-03 and the seismic reflectors of SU-03-2 shows moderate to low reflections near the uplifted region on east-west seismic

line (figure 4) and high amplitude of continuous reflector at juxtaposition of the slope and variable to low amplitude continues towards the low zone in the west, on the same seismic line. Reflectors are parallel to sub-parallel and have high amplitude in the western direction at the bottom of the slope reflectors. The onlapping and downlapping structures of SU-03-2 parasequences form near the platform and the slope, respectively, due to fall of sea level (figure 4). The thickness of SU-03-2 gradually increases towards the basin (westward direction) and abruptly increases towards the southward direction (figures 4 and 5). SU-03-2 isopach map indicates the sediment supply in two directions northeast and north-northeast (figure 6b). The SU-03-2 sequence consists four seismic subunits (U-03-2-1 to U-03-2-4), the lower seismic subunits U-03-2-1 developed in uplifted area and encounters only in F03-04 and F03-02 wells. Seismic subunit U-03-2-2 develops towards the slope and missing in the uplifted region (east) and the basin wards (west) thus not encountered in F02-01, F03-06, F03-04 wells. Seismic subunit U-03-2-3 well developed in overall studied region and encounters in all wells. However, seismic subunit U-03-2-4 developed towards the distal part and encounters in western wells of the study area (figure 7).

The lower seismic subunit U-03-2-1 ($\sim$20 m thick) directly overlaying the SU-02-2 consists of sand to coarse sand (GR funnel shape) indicating prograding parasequences during HST (figure 7). This seismic subunit only comprises of highstand systems tract.

The seismic subunit U-03-2-2 is developed in the middle part of the studied field and it is not encountered in any well (figures 4 and 5). However, this unit visible on seismic sections but the approximate extent has been positioned on well section (figure 7).

U-03-2-3 ($\sim$23 m in well F02-01, $\sim$54 m in F03-06 and $\sim$22 m thick in F03-04) is qualitatively characterized by cylindrical shape geometry of GR log (figure 7), which shows static sea level and aggrading accumulation pattern refers to the period of balance between sediment supply and accommodation space during TST. U-03-2-3 has maximum spatial distribution from east to west and encountered in all wells.

However, the upper seismic subunit U-03-2-4 consists of shale (GR bell shape) indicating retrograding parasequences during TST (figure 7). Afterwards, shale to sand is deposited, which

indicates prograding parasequences during HST. However, in the eastern direction seismic subunit of U-03-2-4 is top lapped prior to reach well F-03-04 (figure 7). Shale (GR bell shape) is deposited due to retrograding pattern of parasequences during TST (figure 7). Later, shale to sand (GR funnel shape) indicates prograding pattern of parasequences during HST.

The overall geometry of SU-03-2 (figure 5) is thickening towards west and forming shallow depression in the uplifted region and displaced in the east by vertical faults. These faults capped by upper boundary of SU-03-2 and disturb the reflections, amplitudes, and continuity of the reflectors due to displacement along the fault.

4.4 *Seismic super unit-04 (SSU-04)*

Seismic super unit-04 includes of two seismic units and five seismic subunits. The upper boundary of SSU-04 is characterized by onlapping of the overlying unit U-05-1-1 (figures 4 and 5).

4.4.1 *Seismic unit-04-1 (SU-04-1)*

The upper boundary of SU-04-1 is characterized by the onlapping of overlying parasequences of U-04-2-1 and the seismic reflectors of SU-04-1 is attributed with low to moderate amplitudes but continuous. SU-04-1 isopach map indicates the sediment supply in two directions east-eastnorth and north-northeast (figure 6b). The thickness of SU-04-1 progressively increases towards the southwestern direction and decreases towards the northeastern direction (figures 4 and 5). The SU-04-1 comprises three depositional sequences (U-04-1-1, U-04-1-2 and U-04-1-3), the lower and upper seismic subunits U-04-1-1 and U-04-1-3 are developed towards the slope and only encounters in western wells F02-01 and F03-06. The middle seismic subunit U-04-1-2 well developed in the studied region and encounters in all wells (figure 7).

Shale to sand (GR funnel shape) is present in the lower seismic subunit U-04-1-1 (~37 m thick deposited during prograding parasequences during LST. Sand to shale (GR bell shape) indicates retrograding parasequences during TST (figure 7). Furthermore, shale to fine sand (GR cylindrical) indicated HST of this seismic subunit deposited during progradational parasequences.

However, the middle seismic subunit U-04-1-2 (~44 m thick) consists of shale to fine sand (GR funnel shape) deposited during prograding parasequences during LST. Shale to sand (GR bell shape) indicates retrograding parasequences during TST (figure 7). Shale to coarse sand (GR cylindrical shape) indicates aggrading parasequences during HST.

The upper seismic subunit U-04-1-3 (~36 m thick) consists of shale to sand (GR bell shape) indicating retrograding parasequences during TST (figure 7). Afterwards, shale to coarse sand (GR funnel shape) indicates prograding parasequences during HST.

4.4.2 *Seismic unit-04-2 (SU-04-2)*

The upper boundary of seismic unit-04-2 is the upper boundary of SSU-04 and the seismic reflectors of SU-04-2 shows low amplitude discontinuous reflection near the uplifted portion and high amplitude continuous reflector towards the slope and developing clinoform geometry (figure 8). Seismic unit-04-2 is bounded from top by onlapping reflectors (angular unconformity) of the overlying parasequences (figures 4 and 5). SU-04-2 comprises of two seismic subunits identified with prominent continuous reflector and GR log behavior in wells F02-01 and F03-06 to the west, F03-02 and F03-04 towards the north and east, respectively (figure 7). The thickness of SU-04-2 is relatively similar in all directions, except northeastern region (platform), where all the sequences are pinching (figures 4 and 5). The lower interval of SU-04-2 (seismic subunit U-04-2-1) is characterized by continuous reflector having high amplitude towards low zone and relatively low amplitudes towards uplifted region. These seismic subunits (U-04-2-1 and U-04-2-2) attributed with high and low amplitude seismic reflections of this interval and correspond to the high and low fluctuations of gamma ray (GR) response, respectively. The reflectors of seismic unit-04-2 show high amplitude facies at the distal part and variable amplitude facies at the proximal and slope of the delta. Closer to the platform, the reflectors are nearly parallel. The downlapping and offlapping of SU-04-2 parasequences indicates the prograding and forestepped accumulation pattern because of the fall of sea level. SU-04-2 isopach map indicates the sediment supply in two directions of northeast (figure 6b). The lower seismic subunit U-04-2-1 (~20 m thick in wells F02-01 and F03-06, this thickness slightly increases toward the slope and reaches up to ~23 m thick in well F03-06)

consists of sand to shale (GR bell shape) indicating retrograding pattern of parasequences during TST (figures 4 and 7). Afterwards, shale to sand (GR funnel shape) indicating prograding pattern of parasequences during HST.

The upper seismic subunit U-04-2-2 (∼20 m thick in well F02-01, ∼33 m thick in F03-06 and decrease down to ∼9 m in well F03-04) consists of shale to sand (GR bell shape) due to retrograding parasequences during TST (figure 7). Followed by shale to sand (GR funnel shape) due to retrograding parasequences during HST. The GR log response suggests that these seismic subunits of SU-04-2 are reducing in thicknesses toward eastern side (well F-03-04) of study area.

4.5 *Seismic super unit-05 (SSU-05)*

Seismic super unit-05 contains two seismic units and 3 seismic subunits. The upper boundary of SSU-05 is marked by toplap structures (figures 4 and 5).

4.5.1 *Seismic unit-05-1 (SU-05-1)*

Upper boundary of SU-05-1 marked on the basis of overlying parasequences onlapping of SU-05-2 and the seismic reflectors of SU-05-1 shows low amplitude continuous reflection in whole studied region. SU-05-1 comprises three seismic subunits (U-05-1-1, U-05-1-2 and U-05-1-3) identified with prominent continuous reflector and GR log behavior in wells F02-01 and F03-06 to the west and F03-02 and F03-04 towards the north and east, respectively (figure 7). These seismic subunits well developed in the western part of the studied area and encounters in all wells (figures 4 and 5). The thickness of SU-05-1 well developed towards the basin (westward direction) and pinching out in eastward direction, although in north-south direction thickness of the sequence is fairly similar (figures 4 and 5). SU-05-1 isopach map indicates the sediment supply in the directions of east-eastnorth (figure 6b).

The U-05-1-1 (∼80 m thick in well F02-01, ∼43 m thick in F03-06 and decrease down to ∼8 m in well F03-04) consists of shale to coarse sand (GR funnel shape) due to prograding parasequences during LST. Coarse sand to shale (GR bell shape) indicating retrograding parasequences during TST (figure 7). Followed by, shale to sand (GR funnel shape) indicating prograding parasequences during HST.

The U-05-1-2 (∼46 m thick in wells F02-01 and F03-06 and decrease down to ∼21 m in well F03-04) interpreted in western region as funnel shape geometry of GR log specifies the shallowing upward strata (shale to sand) and forestepped accumulation pattern of parasequences deposited (prograding strata) during LST. However, in eastern region at the level of platform LST of U-05-1-2 disappeared (figure 7). The bell shape geometry followed by funnel shape geometry of gamma ray (GR) log is identified in all wells. Shale to sand (GR funnel shape) indicating retrograding parasequences during TST. Later, shale to sand (GR funnel shape) is deposited during aggrading parasequences during HST.

The U-05-1-3 (∼42 m thick in well F02-01, ∼38 m thick in F03-06 and decrease down to ∼6 m in well F03-04) interpreted in western region as shale to coarse sand (GR funnel shape) shale (GR funnel shape) indicating retrograding parasequences during TST. Later, shale to sand (GR funnel shape) shows aggrading parasequences during HST.

4.5.2 *Seismic unit-05-2 (SU-05-2)*

The upper boundary of seismic unit-05-2 is the upper boundary of SSU-05 and the seismic reflectors of SU-05-2 shows low amplitude facies at the distal and strong at the proximal. Reflectors are nearly parallel to sub-parallel within this seismic unit. The onlapping of SU-05-2 with the underlying SU-05-1 indicates the retrograding accumulation pattern due to rise of sea level, which is followed by progradation as a result of base level fall marked by truncation of seismic unit-05-2 upper boundary (figures 4 and 5). The thickness of SU-05-2 somewhat increases towards the basin (westward direction) and is approximately similar in north-south direction (figures 4 and 5). SU-05-2 isopach map indicates the sediment supply in the directions of northeast (figure 6b). The SU-05-2 (∼47 m thick and gently decreasing toward east) sequence contains single depositional units and encounters in all wells. This unit consists of fine to coarse sand (GR funnel shape) indicating prograding parasequences during LST. Followed by, fine sand to shale (GR bell shape) shows retrograding parasequences during TST (figure 7). Later, shale to coarse sand (GR funnel shape) shows prograding parasequences during HST.
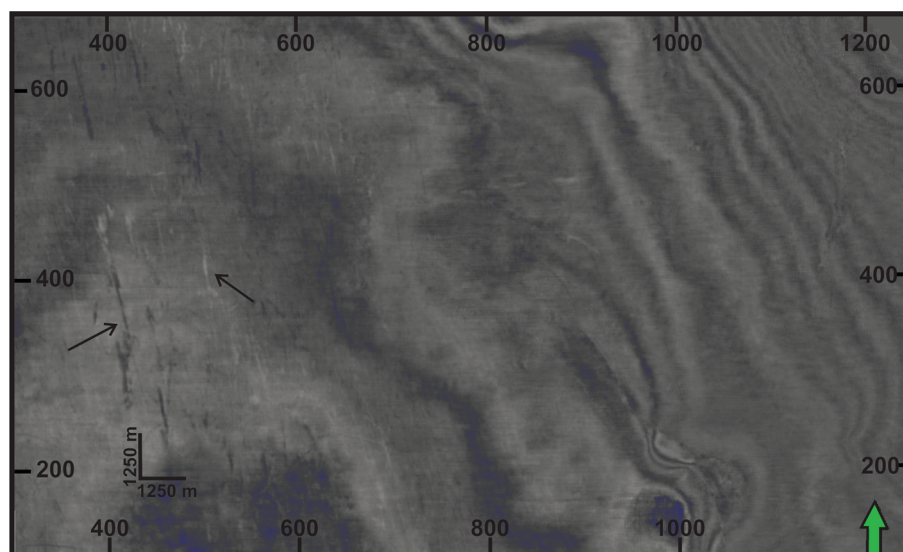
Figure 9. Ice-sheet north–south trending plough-marks observed in the western part of the studied area (time slice 552 ms) almost parallel to the shoreline in the southern Central Graben. The large and continuous glacial lineaments are the fast flowing glacial streams indicated by the black arrow.

5. Regional chronostratigraphy and eustatic significance of unconformities

This study delivers the model of Plio-Pleistocene delta and the stratigraphic relation that exist in southern part of Central Graben Basin, North Sea (figures 9 and 10). The southern-embayment source of sediment influx in Early Pleistocene times was from major European drainage system (Baltic river) and for middle and Late Pleistocene was glacial-fluvial (Moreau *et al.* 2012).

Regionally, in the North Sea region, Sørensen *et al.* (1997) interpreted 9 composite sequences, which include 45 seismic sequences within the Upper Cenozoic time. Different depositional cycles (comprises lowstand, transgressive and highstand systems tracts) were observed in each composite sequence. In the northern embayment 21 sequences were observed due to restricted areal distribution, however almost all 45 sequences were identified in the southern embayment. These composite sequences can be correlated with the Haq *et al.* (1988) chrono-eustatic and chronostratigraphic supercycle sets TEJAS B(TB) and more precisely supercycles TB2 and TB3. Kuhlmann and Wong (2008) expanded the work of Sørensen *et al.* (1997) and divided Mid-Miocene to top Pleistocene interval regionally into 13 seismic units and 18 log units. However, this study predominantly focused on evaluation of Plio-Pleistocene delta, which can add to the chronostratigraphic time lines TB3 of Haq *et al.* (1988).

Sørensen *et al.* (1997) interpreted the climate changes based on fluctuations and the rate of sediment accumulation, which may have been caused by the change of the source area. The studied seismic reflector's maximum inclination towards the southwest and westward direction (lobes/active front of the delta switching) indicates the dominant progradation direction of the delta. SU-01-1 is characterized by the high-angle downlapping internal reflectors at the proximal direction, which results the coarse grained sediments accumulation above and fine sand and shale below. However, at the distal part the internal reflectors are dipping gradually where mainly shale is deposited (figures 4, 5 and 7). The paleo-water depth of SU-01-1 is ranging between few hundred meters (Huuse 2002; Rasmussen *et al.* 2005). Kuhlmann (2004) interpreted temperate, open marine environment of seismic units (SU-01-1 and lower part of SU-01-2) of composite sequence 'V' on the bases of homogeneous pattern of internal reflectors.

The internal reflectors of SU-01-2 appear with onlapping reflection patterns and are restricted in the eastern part of the study area. Kuhlmann and Wong (2008) proposed the model in which the elongated structures were developed on the slope, parallel to the prograding wedges. Based on Kuhlmann and Wong (2008) model the transitional environment (warm and cold environment associated with regression and transgression) of seismic unit (SU-01-2) were interpreted. The study area initially goes under retrogradation and then
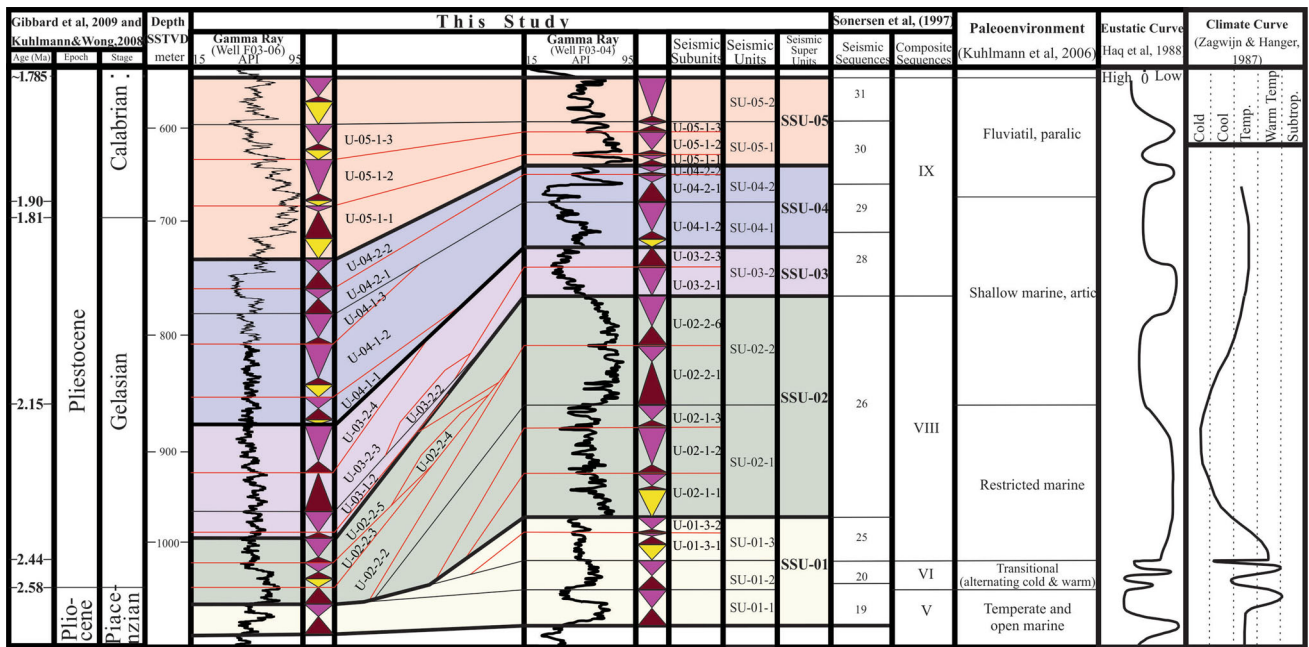
Figure 10. Chronostratigraphic ages acquired after Kuhlmann and Wong (2008) and Gibbard and Head (2009). The seismic super units, seismic units and seismic subunits of the study area correlated with the interpretation of Haq *et al.* (1988), Sørensen *et al.* (1997), and climate interpretation of Zagwijn and Hager (1987). The interpretation of the seismic units and seismic subunits associated with Gamma Ray log of well F03-06 and F03-04. The geometry of U-02-2-4, U-02-2-5 and U-03-2-2 has been detected from the interpreted seismic sections in figures 4 and 5. Haq *et al.* (1988) eustatic sea-level contradicting with Zagwijn and Hager (1987) climate curve in composite sequence IX, due to the increase of sediment influx at the shelf area (where the accommodation space was less during lowstand period) that causes the stratal progradation and eustatic sea-level rise.

aggradation, which is evident in figure 7. Retrogradation indicates the warmer climate condition (rising of sea-level) and/or high influx rate of fine grain sediment accumulation, whereas the aggradation is associated with coarse grain deposits of cold (stable sea level) environment.

The paleoenvironment of SU-01-3 and SU-02-1, which falls within the composite sequence VIII of Sørensen *et al.* (1997), is restricted marine (Kuhlmann and Wong 2008). Each seismic unit parted into hot and cold period of deposition on the basis of GR log deflections (figure 10). The warmer climate at the base of SU-01-3 interpreted by low GR log deflection associated with the coarse grain deposits. On the other hand, high GR log deflection indicates the colder climate conditions associated with the fine grain deposits (figure 7).

Intervals SU-02-2 to SU-04-1 are characterized by the north-south trending lineaments (figure 9). Ottesen *et al.* (2014) observed the ice-sheet ploughmarks (scratches due to iceberg movement) in the northern North Sea Basin. Similar plough-marks have been observed on the time slice 522 m of the studied area. The orientation of lineaments in north to south direction indicates the iceberg movement direction was almost parallel to the

shelf in the southern part of the Central Graben (figure 9). Thick deposition of strata and maximum deflections of gamma ray in terms of retrogradation, progradation and aggradation indicates the environment of deposition of this interval as artic, shallow marine condition (Kuhlmann *et al.* 2006).

The seismic SU-04-2 and SU-05-2 units show initial retrogradation to progradation and then aggradational character and the deposits of high sedimentary influx. On the basis of onlapping of internal reflectors with lower boundaries and toplapping with upper boundaries, paleoenvironment of this interval interpreted as continental and marine (fluvial to paralic) deposits. The reflectors characteristics of SU-04-2 and SU-05-2 infer that probably sedimentation occurred at the time of adequate accommodation space availability during highstand sea level. The thickness of SU-04-2 and SU-05-2 remains approximately similar at the platform but increases towards the basin.

6. Conclusions

This research mainly deals with the detailed analysis of the Plio-Pleistocene deltaic evolution of

North Sea, F3-block. Eleven seismic units and their seismic subunits are being traced and interpreted in detail on the well log and 3D seismic cube data. High-resolution sequence stratigraphy is iteratively applied on wells and seismic date to understand the spatial distribution of seismic units and seismic subunits that are separated by the sequence boundaries and flooding surfaces, respectively. The interpreted seismic units can be correlated with the concept of regional seismo-stratigraphy chrono-eustatic and chronostratigraphic time lines super-cycle sets TEJAS B (TB) and more precisely supercycles TB2 and TB3, which are presented by Haq *et al.* (1988) and Kuhlmann and Wong (2008).

During the Quaternary time, the sedimentation rate of Baltic river significantly increased due to contemporary uplift and accumulation pattern predominantly influenced by the fluvial influx (eroded sediments from the peripheral/hinterland area) and sea-level fluctuations. In the eastern part of F3-block at the level of platform Plio-Pleistocene wave-dominated deltaic sediments mainly consist of coarse sand, sand, fine sand and shale intervals, however in western part towards the slope and basin floor grain size decreases.

Seismic units are divided into seismic subunits based on depositional cycles by gamma ray log trends (funnel shape, bell shape, and cylindrical shape) and the LST, TST and HST stacking geometries. Funnel shape represents (fall of sea-level) prograding parasequence set, developed in both lowstand systems tract (LST) and highstand systems tract (HST). Bell shape represents (rise of sea-level) retrograding parasequence set, developed in transgressive systems tract (TST). Finally, the cylindrical shape represents (no fluctuation on sea-level) aggrading parasequence set, developed in highstand systems tract (HST) and shelf marginal wedge (SMW).

The cutoff values of GR log deflection have been implemented to predict the approximate lithological interpretation. It has been observed that the coarse sand and sand lithologies are mainly associated with the LST and HST conditions; however fine sand and shale are associated with the TST conditions. Maximum flooding surface interpretation is based on maximum GR log deflection within the sequence boundaries.

Pleistocene coastline shifting from north-west to north-south detected by the time structure maps of clinoforms (expanding geometry of offshore delta progradational sequences, toward south-west and west). The younger and restricted seismic units SU-01-3 and SU-02-1of Pleistocene age overstep onto the regionally distributed Late Pliocene (SU-01-1) and Early Pleistocene (SU-01-2) basal seismic units of the delta. Major sea level fall observed in the middle Pleistocene time that is marked by the erosion of SU-02-2 and SU-03-1 at the delta platform and seismic facies shift (progradation) towards the delta slope. Cyclic rise of sea level depicted by the onlapping geometry (aggradation) of seismic facies associated with seismic unit SU-03-2 to SU-05-2.

The paleo-climate of the seismic units is interpreted on the basis of reflectors geometry, rise and fall of sea level and grain size distribution. The warmer climate conditions are associated with the retrogradation pattern, rising sea level and fine grain sediment accumulation, conversely cold climate conditions are delineated by progradation/aggradation, stable/falling sea level and coarse grain sediments deposition.

Acknowledgements

References

Abbink O, Mijnlieff H, Munsterman D and Verreussel R 2006 New stratigraphic insights in the 'Late Jurassic' of the southern central north sea graben and terschelling basin (Dutch offshore) and related exploration potential; *Neth. J. Geosci.-Geol. Mijnb.* **85** 221–238.

Anell I, Thybo H and Stratford W 2010 Relating Cenozoic north sea sediments to topography in southern Norway: The interplay between tectonics and climate; *Earth Planet. Sci. Lett.* **300** 19–32.

Bijlsma S 1981 Fluvial sedimentation from the Fennoscandian area into the north-west European basin during the Late Cenozoic; *Geol. Mijnb.* **60** 337–345.

Benvenuti A, Kombrink H, Veen J H, Munsterman D K, Bardi F and Benvenuti M 2012 Late Cenozoic shelf delta development and mass transport deposits in the Dutch offshore area-results of 3D seismic interpretation; *Neth. J. Geosci.* **91** 591–608.

Catuneanu O, Abreu V, Bhattacharya J, Blum M, Dalrymple R, Eriksson P, Fielding C R, Fisher W, Galloway W and Gibling M 2009 Towards the standardization of sequence stratigraphy; *Earth-Sci. Rev.* **92** 1–33.

Clausen O, Nielsen S, Egholm D and Gołędowski B 2012 Cenozoic structures in the eastern north sea basin-a case for salt tectonics; *Tectonophysics* **514** 156–167.

Clausen O, Nielsen S, Egholm D and Goledowski B 2013 Reply to rasmussen (this volume): Cenozoic structures in the eastern north sea basin – a case for salt tectonics: Discussion; *Tectonophysics* **601** 234–235.

Cloetingh S, Reemst P, Kooi H and Fanavoll S 1992 Intraplate stresses and the post-Cretaceous uplift and subsidence in northern atlantic basins; *Norsk. Geol. Tidssk.* **72** 229–235.

Datta Gupta S, Chatterjee R and Farooqui M Y 2012 Rock physics template (RPT) analysis of well logs and seismic data for lithology and fluid classification in Cambay basin; *Int. J. Earth Sci.* **101(5)** 1407–1426.

Das B and Chatterjee R 2018 Well log data analysis for lithology and fluid identification in Krishna-Godavari Basin, India; *Arab. J. Geosci.* **11** 231–242.

Das B, Chatterjee R, Singha D K and Kumar R 2017 Poststack seismic inversion and attribute analysis in shallow offshore of Krishna-Godavari Basin, India; *J. Geol. Soc. India* **90** 32–40.

De Gans W 2007 *Quaternary*; Geology of the Netherlands, pp. 173–196.

De Jager J 2003 Inverted basins in the Netherlands, similarities and differences; *Neth. J. Geosci.-Geol. Mijnb.* **82** 339–349.

Deagan C and Scull B 1977 A proposed standard lithostratigraphic nomenclature for the central and Northern Sea; *Rep. Inst. Geol. Sci.* 77/25, Bulletin NPD.

Dronkers A and Mrozek F 1991 Inverted basins of the Netherlands; *First Break* **9** 409–425.

Duchesne M J and Gaillot P 2011 Did you smooth your well logs the right way for seismic interpretation? *J. Geophys. Eng.* **8(4)** 514–523.

Duin E, Doornenbal J, Rijkers R, Verbeek J and Wong T E 2006 Subsurface structure of the netherlands-results of recent onshore and offshore mapping; *Neth. J. Geosci.-Geol. Mijnb.* **85(4)** 245–276.

Edgar J A and Van Der Baan M 2011 How reliable is statistical wavelet estimation? *Geophysics* **76(4)** 59–68.

Eidvin T and Rundberg Y 2001 Late Cenozoic stratigraphy of the Tampen area (Snorre and Visund fields) in the northern North sea, with emphasis on the chronology of Early Neogene sands; *Norwegian J. Geol./Nor. Geol. Tid.* **81(2)** 119–160.

Faleide J I, Kyrkjebø R, Kjennerud T, Gabrielsen R H, Jordt H, Fanavoll S and Bjerke M D 2002 Tectonic impact on sedimentary processes during Cenozoic evolution of the northern North Sea and surrounding areas; *Geol. Soc. London. Spec. Publ.* **196** 235–269.

Ghazi S 1992 Cenozoic uplift in the stord basin area and its consequences for exploration; *Nor. Geol. Tid.* **72** 285–290.

Gibbard P L and Head M J 2009 Iugs ratification of the Quaternary system/period and the Pleistocene series/epoch with a base at 2.58 Ma; *Quaternaire* **20** 411–412.

Glennie K W 2009 *Petroleum geology of the North Sea: Basic concepts and recent advances*; Blackwell Science Ltd; Hoboken, New Jersey, United States.

Gregersen U, Michelsen O and Sørensen J C 1997 Stratigraphy and facies distribution of the Utsira formation and the Pliocene sequences in the northern north sea; *Mar. Petrol. Geol.* **14** 893–914.

Haq B U, Hardenbol J and Vail P R 1988 Mesozoic and Cenozoic chronostratigraphy and cycles of sea-level change; In: *Sea-level changes, an integrated approach* (eds) Wilgus C K, Hastings B S, St Kendall C G S C, Posamentier H W, Ross C and Van Wagoner J C, *Soc. Econ. Paleonto. Mineralo. Spec. Publ.* **42** 71–108.

Harding R and Huuse M 2015 Salt on the move: Multi stage evolution of salt diapirs in the Netherlands North Sea; *Mar. Petrol. Geol.* **6** 39–55.

Haszeldine R and Russell M 1987 The Late Carboniferous northern north Atlantic ocean: Implications for hydrocarbon exploration from Britain to the Arctic; *Petrol. Geol. North West Eur.* **2** 1163–1175.

Huuse M 2002 Cenozoic uplift and denudation of southern Norway: Insights from the North sea basin; *Geol. Soc. London Spec. Publ.* **196** 209–233.

Jordt H, Faleide J I, Bjørlykke K and Ibrahim M T 1995 Cenozoic sequence stratigraphy of the central and northern north sea basin: Tectonic development, sediment distribution and provenance areas; *Mar. Petrol. Geol.* **12** 845-879.

Knox R, Bosch J, Rasmussen E S, Heilmann-Clausen C, Hiss M, De Lugt I, Kasinski J, King C, Köthe A and Slodkowska B 2010 Cenozoic; In: *Petroleum geological atlas of the southern Permian basin area* (eds.) Dornenbaal H and Stevenson A, *EAGE Publications, Houten*, 342p.

Kombrink H, Doornenbal J, Duin E, Den Dulk M, Ten Veen J and Witmans N 2012 New insights into the geological structure of the Netherlands; results of a detailed mapping project; *Neth. J. Geosci.* **91** 419–446.

Kooi H, Hettema M and Cloetingh S 1991 Lithospheric dynamics and the rapid Pliocene-Quaternary subsidence phase in the southern north sea basin; *Tectonophysics* **192** 245–259.

Kristoffersen F and Bang I 1982 Cenozoic excl. Danian limestone; In: *Geology of the Danish Central Graben* (ed.) Michelsen O, *Danm. Geol. Undersøg.* **8** 61–70.

Kuhlmann G 2004 High resolution stratigraphy and paleoenvironmental changes in the southern North Sea during the Neogene: an integrated study of Late Cenozoic marine deposits from the northern part of the Dutch offshore area; *Geologica Ultraiectina* **245**, 205p.

Kuhlmann G, Langereis C, Munsterman D, Van Leeuwen R J, Verreussel R, Meulenkamp J and Wong T 2006 Chronostratigraphy of Late Neogene sediments in the southern North Sea basin and paleoenvironmental interpretations; *Palaeogeogr. Palaeoclimatol. Palaeoecol.* **239** 426–455.

Kuhlmann G and Wong T E 2008 Pliocene paleoenvironment evolution as interpreted from 3D-seismic data in the southern North Sea, dutch offshore sector; *Mar. Petrol. Geol.* **25** 173-189.

Lacaze S, Pauget F, Lopez M, Gay A and Mangue M 2011 Seismic stratigraphic interpretation from a geological model – A North Sea case study; SEG Annual Meeting,

Expanded Abstracts, 81st SEG Conference and Exhibition, San Antonio.

Leeder M R 2009 *Sedimentology and sedimentary basins: From turbulence to tectonics*; Wiley-Blackwell, 784p; Hoboken, New Jersey, United States.

Luthi S 2001 Geological well logs: Their use in reservoir modeling; Springer Science and Business Media, 373p; Berlin-Heidelberg, Germany.

Lyngsie S B and Thybo H 2007 A new tectonic model for the Laurentia-Avalonia-Baltica sutures in the North Sea: A case study along Mona Lisa profile 3; *Tectonophysics* **429** 201–227.

Marotta A, Bayer U, Thybo H and Scheck M 2002 Origin of the regional stress in the north German basin: Results from numerical modelling; *Tectonophysics* **360** 245–264.

Miall A 2000 *Principles of sedimentary basin analysis*; Springer-Verlag, 605p; Berlin-Heidelberg, Germany.

Mojeddifar S, Kamali G and Ranjbar H 2015 Porosity prediction from seismic inversion of a similarity attribute based on a pseudo-forward equation (pfe): A case study from the North Sea basin, Netherlands; *Petrol. Sci.* **12** 428–442.

Moreau J, Huuse M, Janszen A, Van Der Vegt P, Gibbard P L and Moscariello A 2012 The glaciogenic unconformity of the southern North Sea; *Geol. Soc. London Spec. Publ.* **368** 99–110.

Munoz A and Hale D 2012 *Automatically tying well logs to seismic data*; CWP, 725p; Colorado School of Mines, Golden, CO80401, USA.

Nelskamp S, Verweij J and Witmans N 2012 The role of salt tectonics and overburden in the generation of overpressure in the Dutch North Sea area; *Neth. J. Geosci.* **91** 517–534.

Ottesen D, Dowdeswell J A and Bugge T 2014 Morphology, sedimentary infill and depositional environments of the Early Quaternary North Sea Basin (56°–62°N); *Mar. Petrol. Geol.* **56** 123–146.

Overeem I, Weltje G J, Bishop-Kay C and Kroonenberg S 2001 The Late Cenozoic eridanos delta system in the southern North Sea basin: A climate signal in sediment supply? *Basin Res.* **13** 293–312.

Qayyum F, Hemstra N and Singh R 2013 A modern approach to build 3D sequence stratigraphic framework; *Oil Gas J.* **111** 46–65.

Rasmussen E, Vejbæk O, Bidstrup T, Piasecki S and Dybkjær K 2005 Late Cenozoic depositional history of the Danish North Sea basin: Implications for the petroleum systems in the Kraka, Halfdan, Siri and Nini fields; *Geol. Soc. London Spec. Publ.* **6** 1347–1358.

Rasmussen E S and Dybkjaer K 2005 Sequence stratigraphy of the upper Oligocene-lower Miocene of eastern Jylland, Denmark: Role of structural relief and variable sediment supply in controlling sequence development; *Sedimentology* **52** 25–63.

Rasmussen E S, Utescher T and Dybkjær K 2013 Drowning of the Miocene billund delta, Jylland: Land-sea fluctuations during a global warming event; *Geol. Surv. Denm. Greenl. Bull.* **28** 9–12.

Rasser M W, Harzhauser M and Anistratenko O 2008 Palaeogene and Neogene; *Geol. Cent. Eur.* **2** 1031–1139.

Ritsema A R and Gurpinar A 2012 Seismicity and seismic risk in the offshore North Sea area; Proceedings of the NATO advanced research workshop, Utrecht, The Netherlands, June 1–4, 1982, Springer Science and Business Media, 420p.

Rohrman M, Andriessen P and Beek P 1996 The relationship between basin and margin thermal evolution assessed by fission track thermochronology: An application to offshore southern Norway; *Basin Res.* **8** 45–63.

Rohrman M, Beek P, Andriessen P and Cloetingh S 1995 Meso-Cenozoic morphotectonic evolution of southern norway: Neogene domal uplift inferred from apatite fission track thermochronology; *Tectonics* **14** 704–718.

Rundberg Y and Eidvin T 2005 Controls on depositional history and architecture of the Oligocene-Miocene succession, northern North Sea basin; *Nor. Petrol. Soc. Spec. Publ.* **12** 207–239.

Sales J 1992 Uplift and subsidence do northwestern Europe: Possible causes and influence on hydrocarbon productivity; *Norsk. Geol. Tidssk.* **72** 253–258.

Schroot B and Schüttenhelm R 2003 Expressions of shallow gas in the Netherlands North Sea; *Neth. J. Geosci.* **82** 91–105.

Sclater J G and Christie P 1980 Continental stretching: An explanation of the post Mid-Cretaceous subsidence of the central North Sea basin; *J. Geophys. Res.* **85** 3711–3739.

Sørensen J and Michelsen O 1995 Upper Cenozoic sequences in the southeastern north sea basin; *Bull. Geol. Soc. Denm.* **42** 74–95.

Sørensen J C, Gregersen U, Breiner M and Michelsen O 1997 High-frequency sequence stratigraphy of upper Cenozoic deposits in the central and southeastern North Sea areas; *Mar. Petrol. Geol.* **14** 99–123.

Spjeldnaes N 1975 Palaeogeography and facies distribution in the Tertiary of Denmark and surrounding areas; *Norges. Geol. Underso.* **316** 289–311.

Steeghs P, Overeem I and Tigrek S 2000 Seismic volume attribute analysis of the Cenozoic succession in the l08 block (southern North Sea); *Glob. Planet. Change* **27** 245–262.

Stuart J Y and Huuse M 2012 3D seismic geomorphology of a large Plio-Pleistocene delta- 'Bright spots' and contourites in the southern North Sea; *Mar. Petrol. Geol.* **38** 143–157.

Tetyukhina D, Van Vliet L J, Luthi S M and Wapenaar K 2010 High-resolution reservoir characterization by an acoustic impedance inversion of a Tertiary deltaic clinoform system in the North Sea; *Geophysics* **75** 57–67.

Thöle H, Kuhlmann G, Lutz R and Gaedicke C 2016 Late Cenozoic submarine slope failures in the southern North Sea evolution and controlling factors; *Mar. Petrol. Geol.* **75** 272–290.

Tigrek S 1998 3D seismic interpretation and attribute analysis of the L08-block, southern North Sea Basin; Unpublished MSc Thesis, Faculty of Applied Earth Sciences, Delft University of Technology, The Netherlands.

Vail P R 1987 Seismic stratigraphy interpretation using sequence stratigraphy, Part 1: seismic stratigraphy interpretation procedure. In: *Atlas of seismic stratigraphy* (ed.) Bally A W, *AAPG Studies in Geology* **27(1)** 1–10.

Vail P R, Mitchum R M and Thompson S 1977 Seismic stratigraphy and global changes of sea level: Part 4. Global Cycles of Relative Changes of Sea Level.: Section 2. Application of Seismic Reflection Configuration to Stratigraphic Interpretation; AAPG, Memoir 26.

Van Dalfsen W, Doornenbal J, Dortland S and Gunnink J 2006 A comprehensive seismic velocity model for the Netherlands based on lithostratigraphic layers; *Netherlands J. Geosci.-Geol. Mijnb.* **85(4)** 277–292.

Van Wees J and Cloetingh S 1996 3D flexure and intraplate compression in the north sea basin; *Tectonophysics* **266** 343–359.

Van Wijhe D V 1987 Structural evolution of inverted basins in the Dutch offshore; *Tectonophysics* **137** 171–219.

Walden A and White R 1984 On errors of fit and accuracy in matching synthetic seismograms and seismic traces; *Geophys. Prospect.* **32** 871–891.

White R 1997 The accuracy of well ties: Practical procedures and examples; 67th Annual International Meeting, SEG Expanded Abstracts, pp. 816–819.

White R and Simm R 2003 Tutorial: Good practice in well ties; *First Break* **21** 75–83.

Winthaegen P and Verweij J 2003 Estimating regional pore pressure distribution using 3D seismic velocities in the Dutch central North Sea graben; *J. Geoch. Expl.* **78** 203–207.

Zagwijn W 1974 The palaeogeographic evolution of the Netherlands during the Quaternary; *Netherlands J. Geosci.-Geol. Mijnb.* **53** 369–385.

Zagwijn W and Hager H 1987 Correlations of continental and marine Neogene deposits in the south-eastern Netherlands and the lower Rhine district; *Meded. Werkgr. Tert. Kwart. Geol.* **24** 59–78.

Ziegler P 1987 Late Cretaceous and Cenozoic intraplate compressional deformations in the Alpine foreland-A geodynamic model; *Tectonophysics* **137** 389–420.

Ziegler P A 1988 Evolution of the Arctic-north Atlantic and the western Tethys-a visual presentation of a series of paleogeographic-paleotectonic maps; *AAPG Memoir* **43** 164–196.

Ziegler P 1990 *Geological atlas of western and central Europe*; Elsevier, Amsterdam, 239.

Ziegler P A and Cloetingh S 2004 Dynamic processes controlling evolution of rifted basins; *Earth-Sci. Rev.* **64** 1–50.

Ziegler P A, Cloetingh S and Van Wees J D 1995 Dynamics of intraplate compressional deformation: The Alpine foreland and other examples; *Tectonophysics* **252** 7–59.

Zouaghi T, Ferhi I, Bédir M, Youssef M B, Gasmi M and Inoubli M H 2011 Analysis of Cretaceous (Aptian) strata in central Tunisia, using 2D seismic data and well logs; *J. Afr. Earth Sci.* **61** 38–61.